

RESEARCH PAPER

## Immobilization of *Saccharomyces cerevisiae* on a natural zeolite for the biosorption of radioisotopes

Meisam Sadeghi<sup>1,\*</sup>, Zahra Moghimifar<sup>2</sup>

<sup>1</sup> Nanotechnology Research Institute, Faculty of Chemical Engineering, Babol Noshirvani University of Technology, Babol, Iran

<sup>2</sup> Faculty of Chemical and petroleum Engineering, Chemistry and Chemical Engineering Research Center of Iran (CCERCI), Tehran, Iran

### ARTICLE INFO

#### Article History:

Received 10 June 2021

Accepted 22 September 2021

Published 15 October 2021

#### Keywords:

Biosorption

*Saccharomyces Cerevisiae*

Uranyl Ion

Zeolite Clinoptilolite

### ABSTRACT

In recent years, intensive attempts have been made to remove toxic heavy metals and radionuclides from wastewater. Uranium is one of the most threatening elements due to its radioactivity and high toxicity. Significant amounts of uranium are released into the environment throughout the nuclear fuel cycle. Biosorption technology offers advantages such as low operating cost and high efficiency for metal removal from aqueous solutions. In this work, the sorption of uranyl ions from aqueous solutions by *Saccharomyces Cerevisiae* (SC) as free cells and in immobilized form on zeolite clinoptilolite was investigated. First, a characterization of the natural zeolite was carried out by classical chemical analysis, XRD, FTIR and TG/DTG, and then the influence of solution pH, temperature, contact time and initial concentration on uranyl sorption was investigated. The concentration range of uranyl in the solution was between 0.02 and 1 mmol L<sup>-1</sup>, which was determined by the inductively coupled plasma optical emission spectrometry (ICP-OES) method. Genetic algorithm and mathematical steps were applied to the membrane bioreactor (MBR) and the results showed that the experimental data matched well with the logistic model. In addition, the immobilization yeast cells of 17.1 × 10<sup>8</sup> cells ml<sup>-1</sup> concentration on clinoptilolite was optimized and observed using a scanning electron microscope (SEM). More results demonstrated that metal binding was carried out extracellularly at the cell wall surface and the rate of uranyl ion sorption by free yeast cells of SC is rapid. The equilibrium adsorption ratio for all samples was calculated, and it was shown that the points corresponding to initial concentrations lower than about 0.1 mmol L<sup>-1</sup> have a higher and closer absorption fraction. Moreover, at concentrations higher than 0.2 mmol L<sup>-1</sup>, the adsorption rate decreases compared to lower concentrations.

#### How to cite this article

Sadeghi M., Moghimifar Z. Immobilization of *Saccharomyces cerevisiae* on a natural zeolite for the biosorption of radioisotopes. *Nanochem Res*, 2021; 6(2):164-177. DOI: 10.22036/ncr.2021.02.004

### INTRODUCTION

Various types of exchangers such as zeolites have widespread and important applications, especially in the nuclear waste recycling industry [1, 2]. Due to the wide distribution of nuclear wastewater and the presence of heavy metals in it, various methods have been used to treat these wastewaters [3-7]. Conventional technologies for reducing heavy metal contamination generally involve one or a

combination of evaporation, chemical separation, and adsorption, ion exchange, and membrane processes [8-10]. When selecting a method for wastewater treatment, various parameters such as the initial cost of the equipment used, the cost of operating the process, minimizing the volume of residual waste and so on are considered [11, 12]. Research results have shown that the use of biological materials is a suitable option both economically and environmentally for the removal

\* Corresponding Author Email: [m-sadeghi@nlai.ir](mailto:m-sadeghi@nlai.ir)

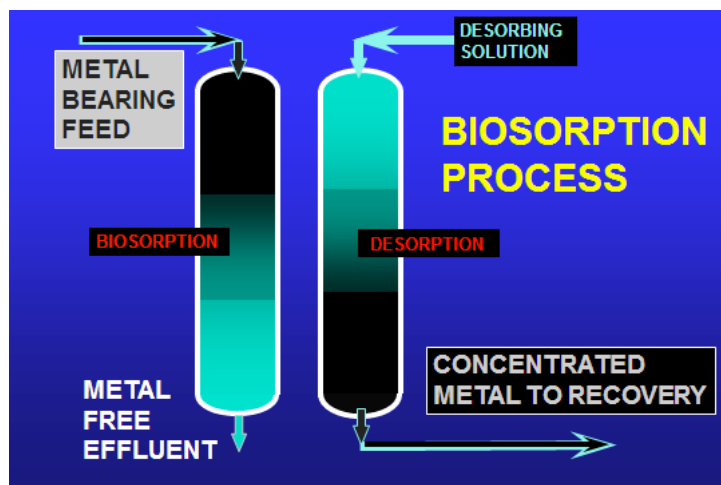


Fig. 1. A molecular scheme for a detailed understanding of the biosorption process

and recovery of heavy metals from aqueous solutions, which is called biosorption technology [13-16]. Biosorption is a property of certain types of non-living microbial biomass to absorb and concentrate heavy metal ions from their very dilute aqueous solution (Fig.1). In summary, the main advantages of this technology are high efficiency at low metal concentrations, performance over a wide range of temperatures and pH, easy recycling of biosorbents, the availability of cheap biomass resources, low cost of adsorption and recycling process [17, 18]. Bacteria, fungi, algae and some plants have different types of biomasses that have good potential for the adsorption of heavy metals [19]. In most separation and purification processes using adsorption technology, a constant bed column with a continuous flow is used [20]. By analyzing the output concentrations of the column against time or volume of the output of the column, the efficiency is obtained with the performance of the fixed bed column [21].

The objective of this study was to remove and recover uranium ions (the major heavy metal in nuclear industry wastewater) by SC, a brown algae species, in a fixed bed column. In this study, a natural zeolite called clinoptilolite from the Semnan mines was selected for the separation of U(VI) ions and characterized by X-ray diffraction (XRD), Fourier-transform infrared spectroscopy (FT-IR) and differential thermal gravimetry (DTG). Furthermore, the influence of variables such as initial concentration, pH and contact time between the exchanger and solution phases on the adsorption of U(VI) ions was investigated and optimized.

## MATERIALS AND METHODS

In this study, yeast from SC was used as a biological adsorbent. The SC strain used in these experiments was PTCC 5052 produced by Collection Center of Scientific and Industrial Research Organization in Iran. Since the microorganism used must maintain its desired properties over time, strain maintenance is very important. To obtain the strain, SC was cultured in a pre-sterilized yeast peptone dextrose (YPD) liquid medium for 48 h at 28 °C. YPD was prepared using 20 g L<sup>-1</sup> peptone (Quelab), 20 g L<sup>-1</sup> glucose monohydrate (Carl Roth), and 10 g L<sup>-1</sup> yeast extracts (Merck) [22]. The zeolite deposit is clinoptilolite and was obtained from the mines of Semnan in the northeastern regions of Iran. The zeolite particles were granulated using standard laboratory sieves in sizes of 425-200 µm, corresponding to a mesh size of 40-70 in the ASTM standard system, and heated at 400 °C for 60 min. After heating, it was cooled to room temperature and kept in a desiccator with silica gel for immobilization and adsorption tests. The heating process was carried out to lose water in the zeolite voids and to prepare the zeolite particles before performing the experimental tests.

## EXPERIMENTAL METHOD

### Preparation of uranyl solution

For the preparation of the uranyl solutions, different types of uranyl stock solution (1 mmol L<sup>-1</sup> UO<sub>2</sub><sup>+2</sup>) were prepared at the required stoichiometric concentration by dissolving different amounts of uranyl nitrate salt (UO<sub>2</sub>(NO<sub>3</sub>)<sub>2</sub>.6H<sub>2</sub>O) in distilled water. The stock solution was used with different

concentrations. The initial pH of the uranyl solution was adjusted to the desired value by adding 0.1 N HNO<sub>3</sub> or 0.1 N NaOH.

#### *Uranyl Equilibrium adsorption experiment before immobilization*

This study was carried out to compare the sorption of free and immobilized cells to evaluate the mechanism of biological sorption process of UO<sub>2</sub><sup>2+</sup> by SC yeast. For comparison, the values used and the test conditions were the same. The concentration of uranyl ions in the solution was determined by inductively coupled plasma optical emission spectroscopy, ICP-OES Optima 7300DV, PerkinElmer, USA.

The sorption (*q*) at equilibrium was calculated for each sample using the following equation:

$$q = V(C_i - C_f) / m$$

Furthermore, the equilibrium absorption percentage was determined using the following equation:

$$EA(\%) = 100(C_i - C_f) / C_i$$

Where *V* is the sample volume (L); *C<sub>i</sub>* and *C<sub>f</sub>* are the initial and final concentrations of uranyl (mmol L<sup>-1</sup>), respectively; *M* is the dry mass of the sorbent (g) and *q* is the amount of ions adsorbed at the equilibrium time per unit mass of the sorbent (mmol g<sup>-1</sup>).

#### *Immobilization of SC*

SC yeast grown in YPD agar medium was first cultured in a 250 ml conical flask containing 50 mL of aseptic YPD culture medium and incubated in a rotary shaker at 28 °C and 160 rpm for 2 days. After that, 1 mL of SC containing 60 mL of aseptic liquid culture solution and 20 mL of zeolite (equivalent to 2.34 g of zeolite) were transferred to 250 mL Erlenmeyer flasks and incubated in a rotary shaker at 25 °C and 130 rpm for 3 days. At this stage, the free yeast cells were transferred to and grow on the zeolite particles. To separate the immobilized cells, a centrifuge was then used at a low speed of 1200 rpm for 20 min. The supernatant was transferred to an aseptic container for cell counting under aseptic conditions and the remainder was stored and dried for 2 days at 50 °C. Then, part of the supernatant from centrifugation of immobilized cells and part of the cells of growth in YPD medium after 2 days

were selected and the number of cells immobilized on the zeolite support was determined by cell counting. It should be noted that to count the number of yeast cells grown for 2 days, due to the large accumulation of cells, the solutions were first diluted 10-fold and 100-fold and counted on the diluted solutions.

#### *Investigation of the mechanism of SC yeast adsorption*

In this section, the mechanism of SC yeast adsorption was investigated. For this purpose, 0.2 L of uranyl solution with an initial concentration of 0.2 mmol L<sup>-1</sup> and pH of 4.5 was prepared and transferred to four Erlenmeyer vessels with a volume of 250 ml. Note also that a control solution was prepared for each of the chemical tests. Then the first sample was considered as the standard solution. To the second sample, 20 ml of crude culture medium (before adding biomass) was added. Similarly, 20 mL of supernatant after biomass centrifugation and 20 mg of dry adsorbent (used in the equilibrium adsorption tests) were added to the third and fourth samples and proceeded as in the previous experiments. The volume of 20 mL corresponds to the 20 mg of adsorbent, which can be calculated by the density of the supernatant and the culture medium were measured with a tensiometer.

#### *Uranyl Equilibrium adsorption experiment after immobilization*

Where, *q* is the mmol of adsorbed uranyl ions per gram of fixed yeast adsorbent calculated from the following formula:

$$q = V(C_{f(\text{blank})} - C_f) / m$$

Where *C<sub>f(blank)</sub>* is the equilibrium concentration of uranyl after adding crude zeolite to the solution and *C* is the equilibrium concentration of uranyl after adding the cell immobilized on the zeolite to the solution.

#### *Genetic algorithm for biosorption process*

The genetic algorithm is applied to obtain the optimal parameter values by minimizing the output error between the experimental and simulation output data. This section deals with the estimation of parameters for the growth of SC in MBR. In this work, mathematical modeling techniques were applied to study the sorption of UO<sub>2</sub><sup>2+</sup> in the MBR operating system in batch mode. The model

Table 1. Mathematical models for MBR

		Parameters
Mathematical Models	Logistic	$\frac{dx}{dt} = \left[ K \cdot \left( 1 - \frac{x}{x_m} \right) + \frac{F_m}{V_0 - F_m \cdot t} \right] \cdot X$
		$\frac{ds}{dt} = -K \cdot \left( 1 - \frac{x}{x_m} \right) \cdot \frac{X}{Y_{x/s}} + \frac{F_m}{V_0 - F_m \cdot t} \cdot S$
		$\frac{dp}{dt} = K \cdot \left( 1 - \frac{x}{x_m} \right) \cdot X \cdot Y_{p/s} + \frac{F_m}{V_0 - F_m \cdot t} \cdot (p - p_m)$
	Tessier	$\frac{dx}{dt} = \left[ \mu \cdot \left( 1 - \exp \left( -\frac{S}{K} \right) \right) + \frac{F_m}{V_0 - F_m \cdot t} \right] \cdot X$
		$\frac{ds}{dt} = -\mu \cdot \left( 1 - \exp \left( -\frac{S}{K} \right) \right) \cdot \frac{X}{Y_{x/s}} + \frac{F_m \cdot S}{V_0 - F_m \cdot t}$
$\frac{dp}{dt} = \mu \cdot \left( 1 - \exp \left( -\frac{S}{K} \right) \right) \cdot X \cdot Y_{p/s} + \frac{F_m \cdot (p - p_m)}{V_0 - F_m \cdot t}$		
Monod	$\frac{dx}{dt} = \left[ \frac{\mu_m \cdot S}{K_s + S} + \frac{F_m}{V_0 - F_m \cdot t} \right] \cdot X$	
	$\frac{ds}{dt} = -\frac{\mu_m \cdot S \cdot X}{(K_s + S) \cdot Y_{x/s}} + \frac{F_m \cdot S}{V_0 - F_m \cdot t}$	
	$\frac{dp}{dt} = \frac{\mu_m \cdot S}{K_s + S} \cdot X \cdot Y_{p/s} + \frac{F_m \cdot (p - p_m)}{V_0 - F_m \cdot t}$	
Moser	$\frac{dx}{dt} = \left[ \frac{\mu_m \cdot S^n}{K_s + S^n} + \frac{F_m}{V_0 - F_m \cdot t} \right] \cdot X$	
	$\frac{ds}{dt} = -\frac{\mu_m \cdot S^n \cdot X}{(K_s + S^n) \cdot Y_{x/s}} + \frac{F_m \cdot S^n}{V_0 - F_m \cdot t}$	
	$\frac{dp}{dt} = \frac{\mu_m \cdot S^n}{K_s + S^n} \cdot X \cdot Y_{p/s} + \frac{F_m \cdot (p - p_m)}{V_0 - F_m \cdot t}$	
Contois	$\frac{dx}{dt} = \left[ \frac{\mu_m \cdot S}{K_s \cdot X + S} + \frac{F_m}{V_0 - F_m \cdot t} \right] \cdot X$	
	$\frac{ds}{dt} = -\frac{\mu_m \cdot S \cdot X}{(K_s \cdot X + S) \cdot Y_{x/s}} + \frac{F_m \cdot S}{V_0 - F_m \cdot t}$	
	$\frac{dp}{dt} = \frac{\mu_m \cdot S}{K_s \cdot X + S} \cdot X \cdot Y_{p/s} + \frac{F_m \cdot (p - p_m)}{V_0 - F_m \cdot t}$	

describes cell growth, substrate concentration, and  $UO_2^{2+}$  sorption. The mathematical model was derived from the principles of mass and energy balance. Therefore, the mass balance was first applied around the bioreactors and the general differential equations describing the concentration of  $UO_2^{2+}$  sorption, consumed glucose substrate and microorganism SC were set up as a function of time and dilution rate in batch and continuous modes, respectively. The mathematical modeling was based on the kinetic models of the Logistic, the Tessier, the Monod, the Moser and the Contois. The obtained mathematical models for the MBR bioreactor

are summarized in Table 1. The proposed kinetic models were applied to the obtained equations and the coefficients corresponding to the proposed models were considered as variables and optimized. The final equations describing the batch operation, consisting of 7 to 9 variables with respect to the applied model, were solved simultaneously using a genetic algorithm.

*Optimization of Uranyl Equilibrium adsorption experiment*

*(a) Effect of time*

50 mL solutions with a concentration of 0.2

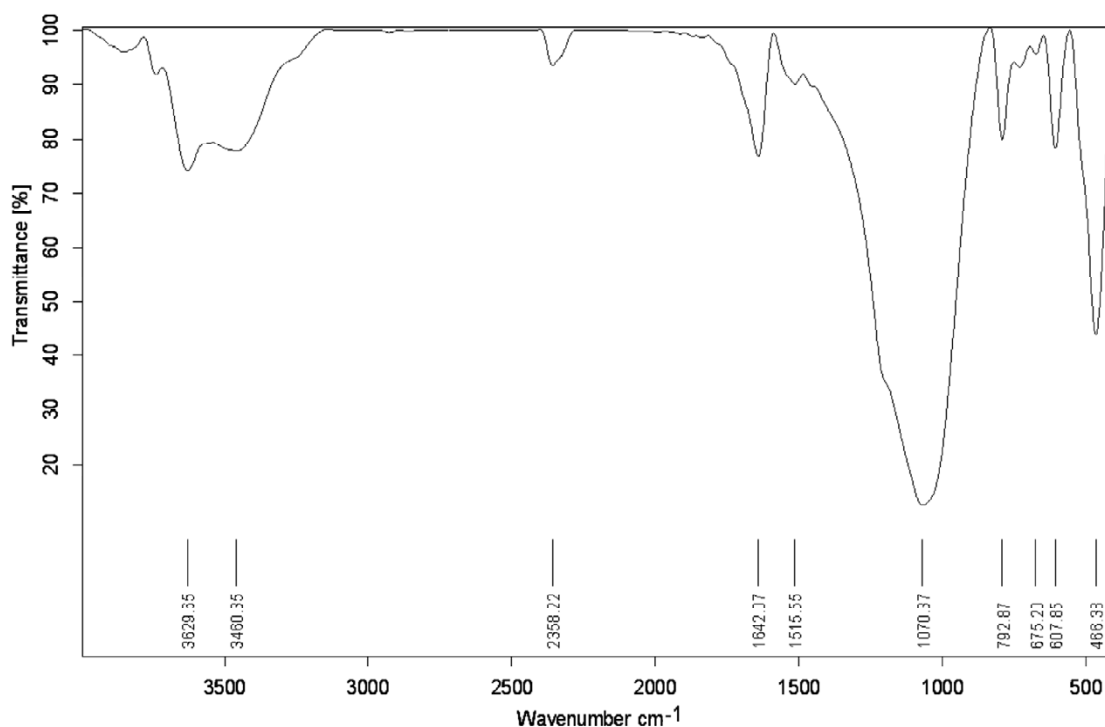


Fig. 2. FT-IR spectrum of zeolite type of clinoptilolite

mmol L<sup>-1</sup> uranyl from standard uranyl solution were prepared. The pH and temperature of the solution were adjusted to 4.5 and 25 °C, respectively. By adding 20 mg of yeast adsorbent to the solutions, the samples were incubated at 200 rpm for a contact time of 6 h. The samples were incubated at 200 rpm. Then, to separate the adsorbed uranyl ions, the supernatant was centrifuged at a speed of 9000 rpm for 10 min. Finally, the time dependence of uranyl biosorption on the immobilized biomass was investigated.

(b) *Effect of temperature*

50 mL uranyl solutions with an initial concentration of 0.2 mmol L<sup>-1</sup> were prepared. The solutions were adjusted to a pH of 4.5. Then, 20 mg of yeast adsorbent was added to the solutions and incubated for 3.5 h at different temperatures ranging from 20 °C to 40 °C to study the uranyl sorption. After filtration of the mixture, the filtrate containing uranyl ions was measured.

(c) *Effect of pH*

50 mL of uranyl solutions with an initial concentration of 0.2 mmol L<sup>-1</sup> were prepared. Then 20 mg of yeast adsorbent for uranyl removal was added to the solutions at different pH range from 3

to 6 and the optimum pH was determined.

(d) *Effect of initial uranyl ion concentration*

50 mL of uranyl solutions with initial concentrations ranging from 0.02 to 1 mmol L<sup>-1</sup> at an optimum pH of 4.5 were prepared. Then 20 mg of yeast adsorbent was added and the effect of initial uranyl ion concentration was studied.

*BET analysis*

To observe the effect of cynoptilot zeolite on the specific surface area of biomass, the BET assay was performed for the primary biomass and the modified biomass (absorbed cells on zeolite), respectively.

**RESULTS AND DISCUSSIONS**

*Characterization of clinoptilolite*

Fig. 2 shows the FT-IR spectrum of the zeolite clinoptilolite sample. The spectra in the range of 400-800 cm<sup>-1</sup> indicate symmetrical tensile vibrations. The strong band observed at 1070 cm<sup>-1</sup> is due to the tensile vibration of Si-(Al)-O bond in the quadrangle of Si(Al)O<sub>4</sub>. The band appearing around 1515 cm<sup>-1</sup> is devoted to the asymmetric tensile vibrations of Al-O or Si-O bond. The bending vibrations of water molecules appear at 1642 cm<sup>-1</sup>.

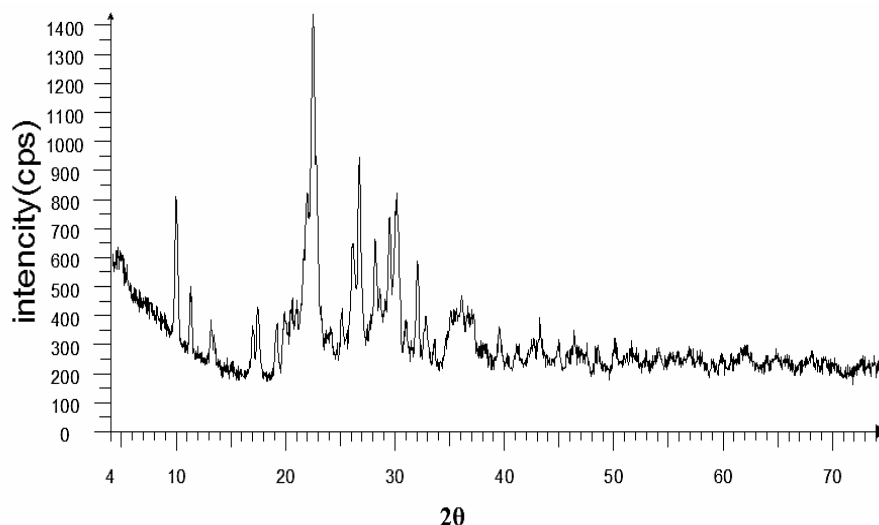


Fig. 3. XRD spectrum of zeolite type of clinoptilolite

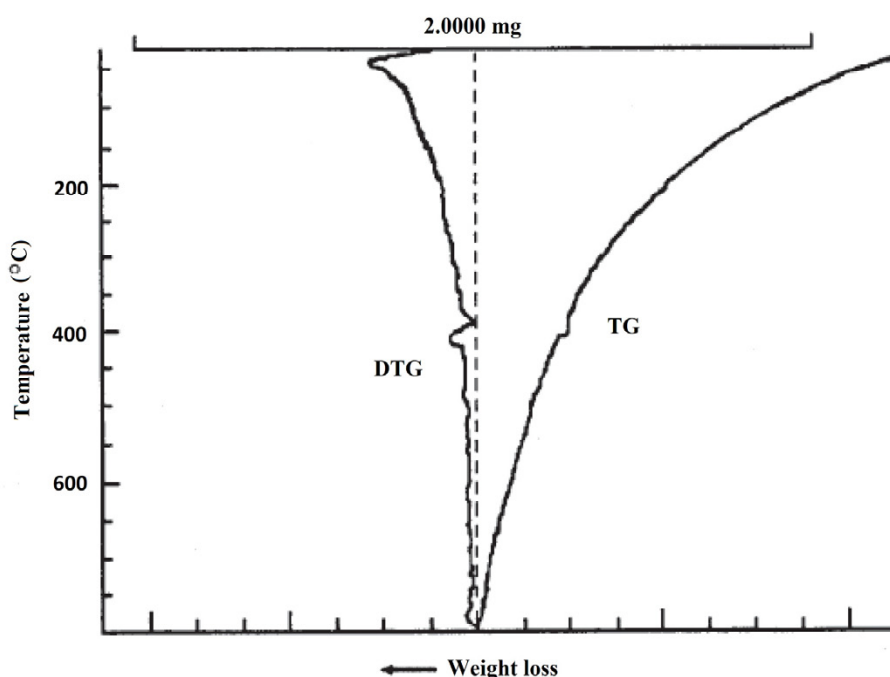


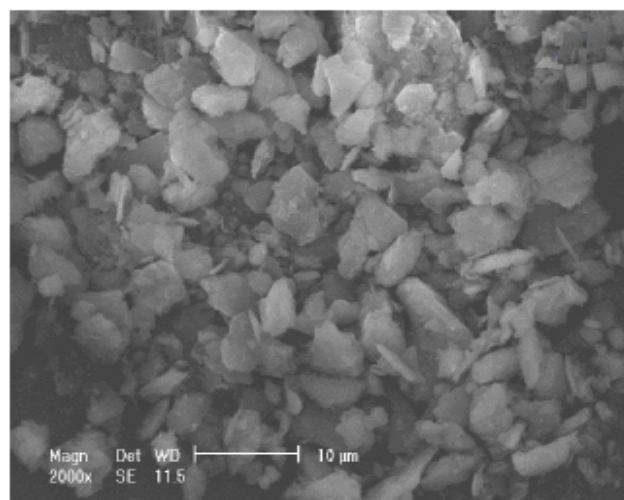
Fig. 4. DTG/TG spectrum of zeolite type of clinoptilolite

The broadband peak in the range of  $3400\text{--}3700\text{ cm}^{-1}$  is assigned to hydroxyl groups, with the spectrum at  $3460\text{ cm}^{-1}$  assigned to Si-(OH)-Al and Si-OH, and the spectrum appearing at  $3629\text{ cm}^{-1}$  is usually for Brønsted acid.

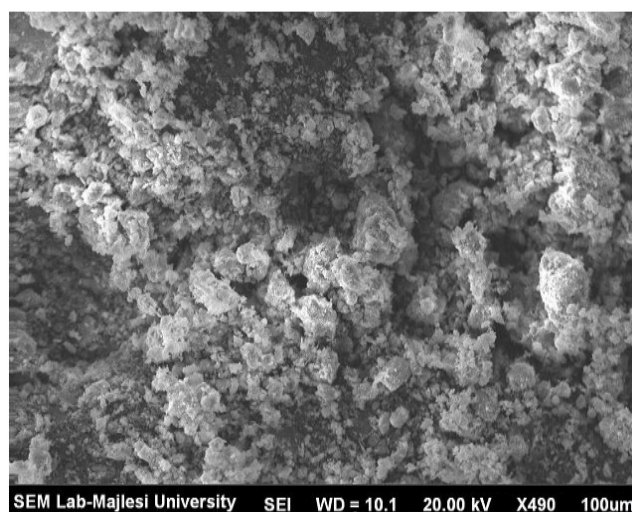
In Fig. 3, the structure of zeolites was studied using X-ray spectroscopic images from  $2\theta = 4^\circ$  to  $2\theta = 70^\circ$ . Thus, noses of  $2\theta$  times 9.63, 22.40, 26.71, 30.19 and 32.74 degrees were observed in zeolite

clinoptilolite assigned to biotite, clinoptilolite, quartz, feldspar and dolomite, respectively.

Moreover, thermal decomposition method was used to measure the amount of water and other volatiles in the samples by reducing the weight of the sample. The temperature range studied was from 25 to  $900^\circ\text{C}$  and the rate of temperature changes was  $10^\circ\text{C min}^{-1}$ . The thermal curve for natural zeolite of clinoptilolite is shown in Fig. 4.



(a)



(b)

Fig. 5. (a) Scanning electron micrograph of natural clinoptilolite (b) Scanning electron micrograph of clinoptilolite with immobilized yeast cells

An index peak can be seen in the temperature range of 25-200 °C, which shows a percentage weight loss of 1.13%. The current weight loss is due to the removal of water molecules. In this range, weakly bound water molecules are released. The escape of water molecules is very rapid, which can be clearly seen. In the temperature range between 200 and 300 °C, the slope of the thermocurve decreases. The escape of water is slower, but it is continuous. Above 400 °C this speed slows down even more, and gradually water molecules leave the zeolite bed. In practice, the amount of water leaving the zeolite structure can be a good criterion for the adsorption capacity, since the released water molecules can be

given to other molecules. As a result of heating the sample, the water molecules, trapped in the zeolite channels and cavities as well as the adsorbed water molecules, are expelled from the system.

#### *Immobilization of yeast cells on clinoptilolite*

The characterization of the zeolite surface is determined by SEM. The detector of type Secondary Electron Imaging (SEI) was used for imaging SEM (Fig. 5).

Fig. 5a shows the images of the crystalline structure of the acid-leached zeolite without cells and Fig. 5b represents the morphology of the zeolite loaded with cells. A comparison of Figs. 5a

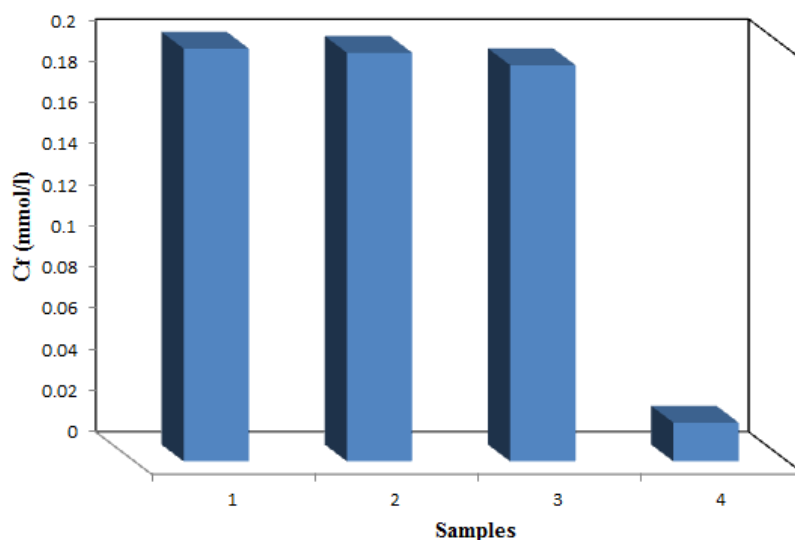


Fig. 6. Diagram related to the mechanism of adsorption under the above conditions.

Table 2. Kinetic mathematical model parameters for MBR

Parameters		Ksp (gL <sup>-1</sup> )	Kss (gL <sup>-1</sup> )	Ksx (gL <sup>-1</sup> )	μ <sub>m</sub> (h <sup>-1</sup> )	R <sup>2</sup>
Mathematical Models	Logistic	0.98	1.321	0.47	15.67	0.9958
	Tessier	15.02	28.94	22.08	0.49	0.9904
	Monod	13.02	17.46	8.99	0.47	0.9874
	Moser	25.85	28.43	42.53	1.40	0.9912
	Contois	9.09	11.30	29.66	0.58	0.9801

and 5b indicates that the surface structure of the zeolite has changed and the voids in the zeolite have become loaded with cells. The proliferation of yeast cells growing on the zeolite support was clearly preserved. In summary, the SEM photos confirm the main assumptions of this study that the trapped nutrients above the cavities were used by the immobilized SC cells for biomass production. The calculated number of immobilized SC cells per support was  $17.1 \times 10^8$  cells ml<sup>-1</sup>.

#### Mechanism of SC yeast adsorption

The density of the culture medium and supernatant was determined using a tensiometer as 1.032 g/ml and 1.039 g/ml, respectively. In Fig. 6, the amount of uranyl ions in the solutions after centrifugation was shown. As shown in Fig. 6, sample 1 is a standard control solution used as a basis for comparison. The final amount of uranyl ions in sample 2 was reduced by only 1% and in sample 3 by 4%, so the sorption of uranyl ions was not due to the materials in the culture medium or supernatant. In sample 4, the uranyl ion sorption rate is 9.1% of sample 1; therefore, it can be

concluded that the sorption of uranyl ions by SC is due to the surface of the cell wall. Additionally, due to the fact that the adsorption reaches equilibrium in a short time, the adsorption of the adsorbent and cation by washing with sodium carbonate solution is easy, so the adsorption has been extracellular.

#### Genetic algorithm for biosorption process

The results of the kinetic models used, i.e. the Logistic, the Monod, the Moser, the Tessier and the Contois models, were in good agreement with the experimental data (Table 2). Among the considered models, the logistic model showed the best performance for MBR in batch mode with a regression value of 0.9958. Considering the obtained results, which are closely comparable with the experimental data, the models used with the optimized coefficients can be efficiently used to predict the concentrations of the different components involved in UO<sub>2</sub><sup>2+</sup> sorption using glucose substrate and SC microorganisms (Fig. 7). The great advantage of this technique is the ability of the applied models to predict the behavior of the system without experimental studies.

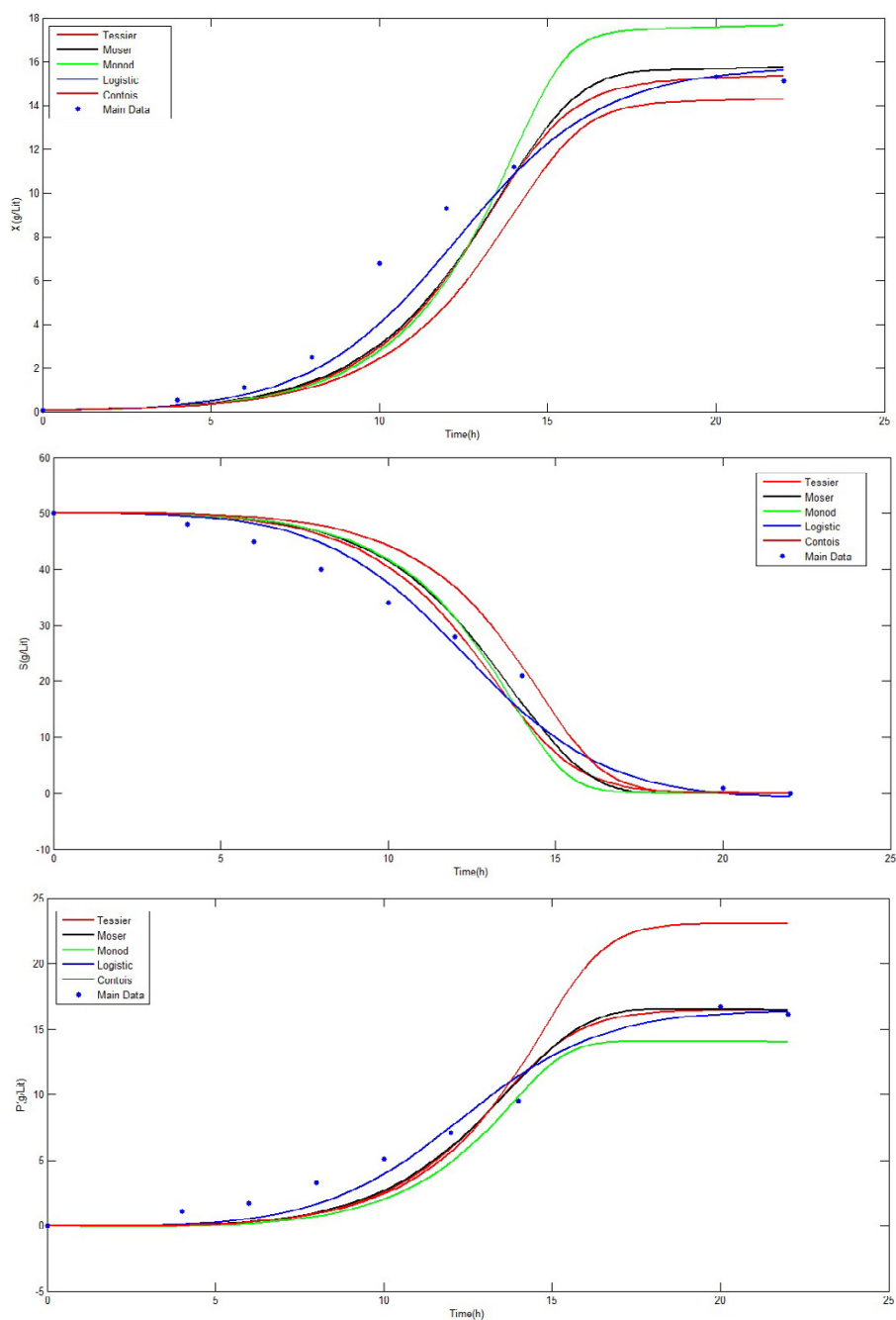


Fig. 7. Prediction of the different models for (a) microorganisms, (b) substrates and (c) biosorption product in batch membrane reactors

*Optimization of uranium ion adsorption using free and immobilized yeast adsorbent*

*(a) Influence of time*

The effect of time on the equilibrium adsorption capacity of bio-modified clinoptilolite for  $UO_2^{2+}$  ions was investigated. The biosorption of metal

ions from solution is rapid at the initial stage. Fig. 8 shows a plot of biosorption against time.

The results demonstrate that the biosorption of uranyl ions is rapid and  $UO_2^{2+}$  ions are removed up to 90% in the first 30 minutes of sorption. The rapid phase is probably due to the high number of

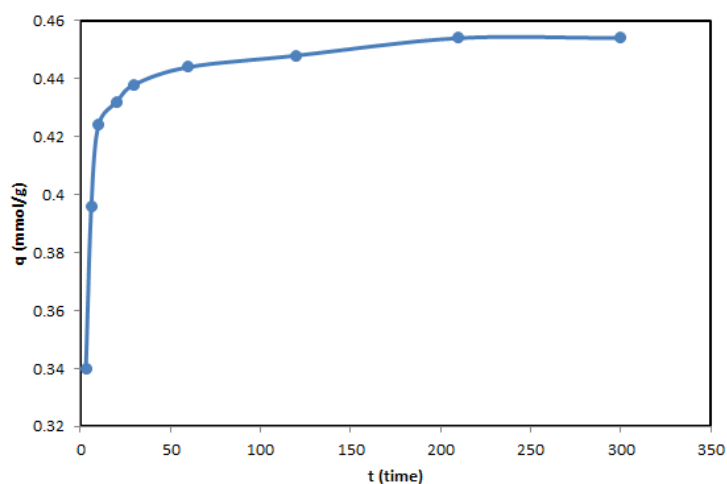


Fig. 8. Diagram of equilibrium uranium ion adsorption as a function of time

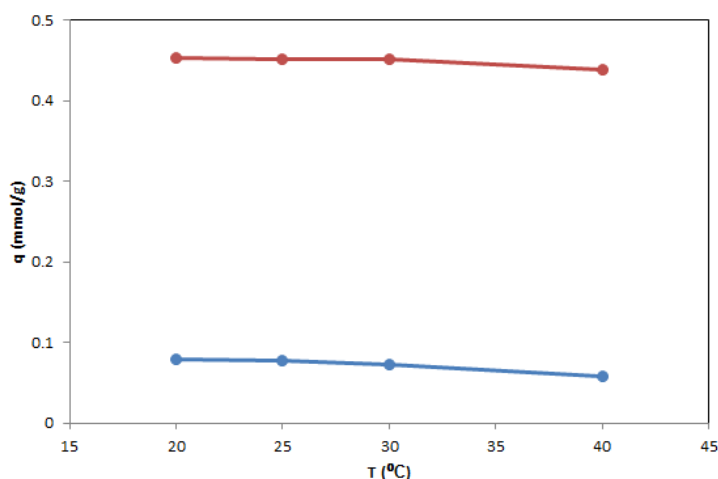


Fig. 9. Diagram of equilibrium uranium ion adsorption as a function of temperature

available active adsorption sites on the biomass cell wall. When the active binding sites were saturated with time, a slowdown was achieved. Thereafter, equilibrium was established in 4 h and this time was chosen as the contact time for further experiments.

*(b) Influence of temperature*

Fig. 9a, shows the sorption of  $UO_2^{2+}$  ions at pH = 4.5 and a temperature range of 20-40 °C with a constant initial concentration of 0.2 mmol  $L^{-1}$  against temperature. The results showed that temperature has no significant effect on the sorption capacity of uranyl. The heat of adsorbent is one of the most important process variables, which can be expressed by energy dependent mechanisms. However, the energy-independent

mechanisms are less affected by temperature. Considering these results, these processes may be responsible for biosorption and seem to be largely physicochemical in nature.

Moreover, investigation of the effect of temperature on the sorption of uranyl by immobilized yeast cells at the above temperatures in Fig. 9b demonstrates that as the temperature increases, the adsorption rate decreases, indicating that the adsorption process by the immobilized cells of SC is exothermic. As the zeolite cavities expand with increasing temperature, the equilibrium concentration of urea ion decreases after adding the crude zeolite to the solution, but the equilibrium concentration of urea ion does not change significantly after adding the immobilized

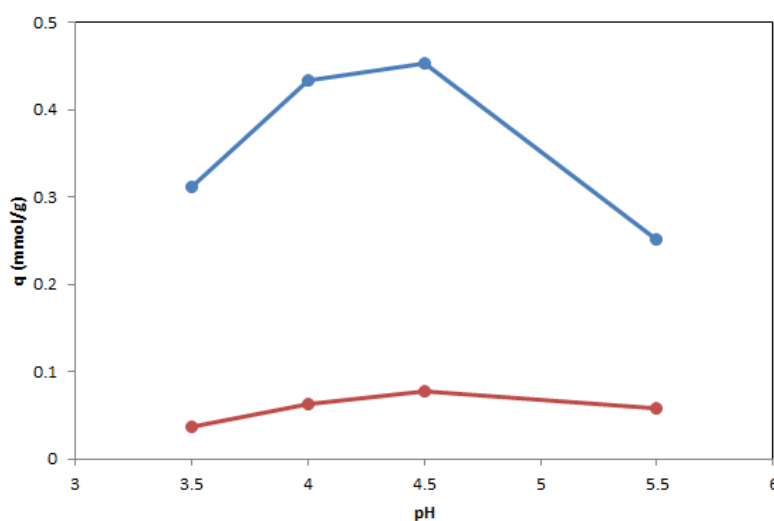


Fig. 10. Diagram of equilibrium uranium ion adsorption as a function of pH

cell on the zeolite. Therefore, as the temperature increases and the equilibrium concentration difference decreases, the amount of adsorption decreases as well. This indicates that the adsorption structure in the immobilized state does not change significantly with increasing temperature up to about 40 °C.

#### (c) Influence of pH

The influence of pH on  $\text{UO}_2^{2+}$  adsorption capacity by the sorbent is shown in Fig. 10a. The interaction of the cell wall groups containing carboxyl, amine and amide groups with the uranyl ion in solution was dependent on the amount of protonated functional group present on the biosorbent, which in turn depends on the pH. According to the two results obtained by the pH-dependent protonation status of the functional groups on the cell surface and the type of metal species present in the solution, pH = 4.5 was chosen as the optimum pH for uranyl biosorption. Moreover, several studies on uranium sorption by different types of adsorbents showed that a similar adsorption behavior in the defined pH range.

When the effect of pH on the sorption of uranyl ions by immobilized SC cells was investigated, pH = 4.5 was again determined for maximum adsorption (Fig. 10b). But in this case, the changes of adsorption against pH are not significant compared to free cells.

#### (d) Influence of initial uranyl ion concentration

The initial concentration dependence of  $\text{UO}_2^{2+}$  adsorption by the sorbent is shown in Fig. 11.

At low concentrations of  $\text{UO}_2^{2+}$ , the adsorption increases rapidly with increasing concentration. At high concentrations, the adsorption rate increases slowly. Finally, the adsorbent is saturated due to an increase in  $\text{UO}_2^{2+}$  concentration. This is due to the fact that the suitable active sites gradually decrease with increasing uranyl ions.

Next, the effect of initial solution concentration on uranyl ion sorption by immobilized SC cells on zeolite support was investigated. As shown in Fig. 12, the adsorption rate of metal ions increases relatively steeply at low concentrations. At high concentrations, the adsorption rate increases with a small slope as the available active sites gradually decrease with increasing concentration.

#### Calculation of the equilibrium absorption ratio

The percentage of equilibrium adsorption for all samples was calculated using the equation and its graph was plotted. As can be seen in Fig. 13, the points corresponding to initial concentrations of less than about 0.1 mmol L<sup>-1</sup> have a higher and closer absorption percentage. Also, in this concentration range, the difference between the initial and equilibrium concentrations ( $C_i - C_f$ ) is closer to the value of  $C_f$  due to the very small amount of  $C_i$ , which indicates higher adsorption and can be clearly seen in the Fig. 14. However, at concentrations above 0.2 mmol L<sup>-1</sup>, the adsorption rate decreases compared to low concentrations.

#### BET analysis

Comparing the results from BET for the

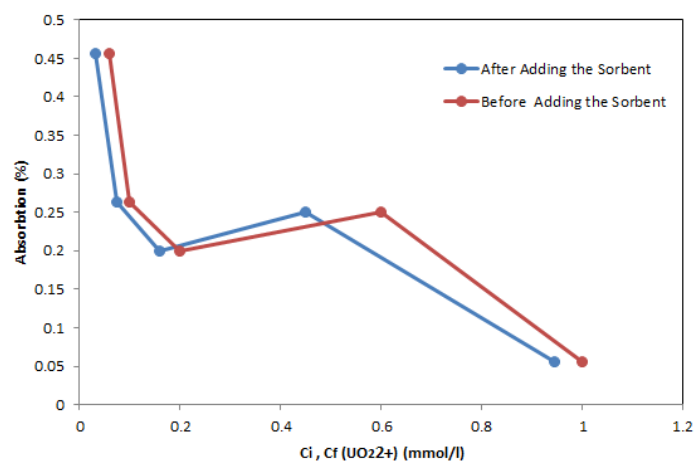


Fig. 11. Equilibrium sorption of uranyl ions by SC yeast as a function of the initial concentration (before addition of the adsorbent) and the final concentration of uranyl ions (after addition of the adsorbent) in the solution

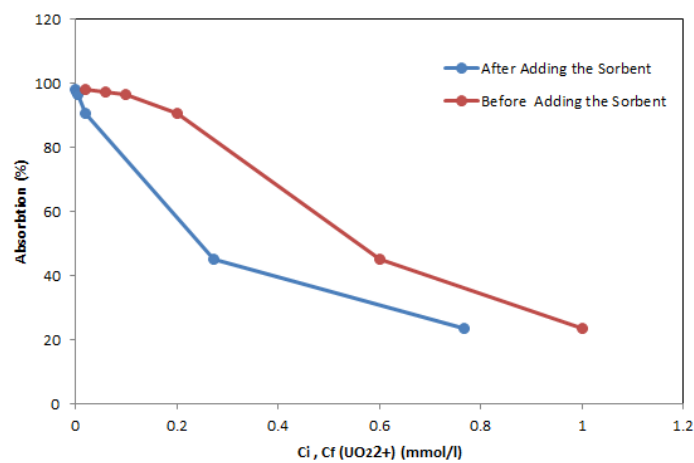


Fig. 12. Equilibrium sorption of uranyl ions by immobilized SC yeast adsorbent as a function of the initial concentration (before adding the adsorbent) and the final concentration of the uranyl ion (after adding the adsorbent) in the solution

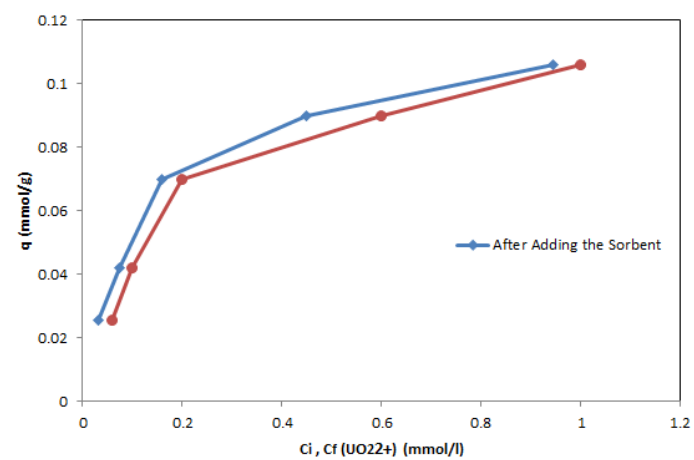


Fig. 13. Equilibrium data of uranyl ions by SC yeast adsorbent under the condition of PH = 4.5, temperature of 25 ° C, 50 mL initial volume of solution, 20 mg immobilized SC yeast adsorbent and equilibrium time of 3.5 hours

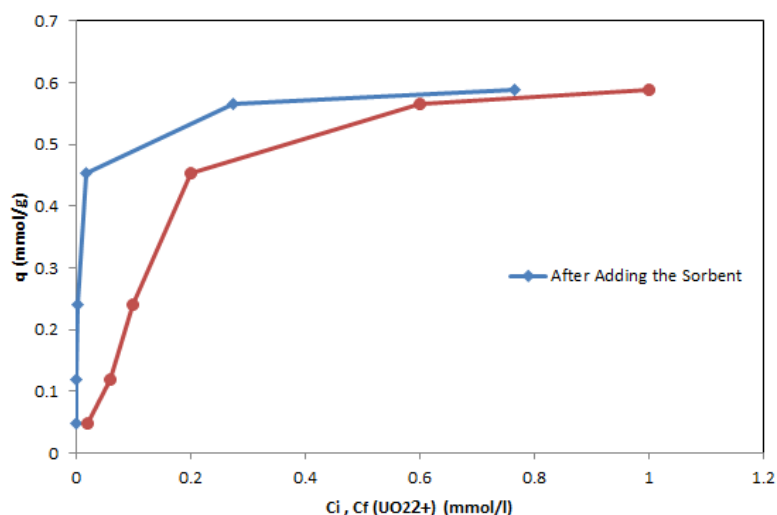


Fig. 14. Equilibrium data of uranyl ions by immobilized SC yeast adsorbent under the condition of PH = 4.5, temperature of 25 ° C, 50 mL initial volume of solution, 20 mg immobilized SC yeast adsorbent and equilibrium time of 3.5 hours

Table 3.

Samples	Total pore volume (cm <sup>3</sup> /gr)	Surface area (m <sup>2</sup> /gr)	average hole diameter (nm)
Clinoptilolite	0.1062	36.06	11.78
SC - Clinoptilolite	0.0673	12.67	2.26

primary and modified biomass shows an increase in the surface area of the modified biomass as a result of adsorption to clinoptilolite zeolite. Due to the fact that the original biomass area was smaller than the minimum standard value of the BET test, the instrument received no response.

After the biomass correction, the specific surface area obtained from the BET test was equal to  $9.688 \times 10^{-3} \text{ m}^2/\text{g}$ ; the average porosity diameter was equal to  $1.619 \times 10^2 \text{ nm}$  and the total porosity was equal to  $3.922 \times 10^{-4} \text{ cm}^3/\text{g}$ .

As can be seen from the data in Table 3, the total pore volume and average pore diameter of the modified zeolite adsorbent decreased significantly compared to the clinoptilolite zeolite. The placement of yeast molecules in voids in the zeolite structure (which in turn reduces the volume of the voids and consequently reduces the diameter of the void) together with the placement of yeast molecules on the surface of the zeolite, reduce the surface area of the effective zeolite sites. For this reason, the surface area of the modified zeolite is much smaller than that of the clinoptilolite zeolite, and this could be a justification for the proper modification of the crude zeolite surface and the placement of yeast molecules in the sites.

## CONCLUSIONS

Based on the results, it was found that SC yeast cells can be immobilized based on natural zeolite clinoptilolite. It was also found that the biosorbent used is suitable for the adsorption of uranyl ions from aqueous solutions. The adsorption mechanism was carried out by forming a complex of polysaccharide and carboxyl groups on the cell wall of yeast by metal cations and ion exchange in the form of adsorption on the cell wall and deposition in the solution. Metal binding was also carried out extracellularly at the cell wall surface.

Moreover, a genetic algorithm is applied to obtain the optimal parameter values and consider the parameter estimation for the growth of SC in MBR. The results of the logistic kinetic model showed a very satisfactory agreement with the experimental data. The results of the discontinuous method showed that the rate of uranyl ion sorption by free yeast cells of SC is rapid, such that 85% of the total sorption occurs in the first 10 min of contact, allowing the use of economical low-volume reactors with high efficiency. Temperature has little effect on the uranium ion sorption process by free and immobilized yeast cells, but its effect is somewhat more pronounced in the immobilized

state than in the free cell state.

The results of BET technique showed that the total pore volume and average pore diameter decreased for modified clinoptilolite zeolite. Furthermore, a slight decrease in adsorption with increasing temperature indicates that the adsorption process is exothermic. The best pH for the adsorption process was found to be 4.5. By changing the pH, the amount of adsorption in the free cell state decreases more than the adsorption by immobilized cells. The increase in the adsorption capacity of clinoptilolite after immobilization allows a better use of this adsorbent in columnar systems. Moreover, due to the high mechanical strength of this adsorbent compared to free cells, it will perform better with multiple desorption/adsorption periods in continuous systems. In addition, the cheapness as well as high porosity and high specific surface area of natural zeolite make clinoptilolite exceptional.

#### ACKNOWLEDGEMENTS

None. No funding to declare.

#### CONFLICT OF INTEREST

All authors have no conflicts of interest to declare.

#### REFERENCES

- [1] Yang J, Volesky B. Modeling Uranium-Proton Ion Exchange in Biosorption. *Environmental Science & Technology*. 1999;33(22):4079-85.
- [2] Liu H, Wang R, Jiang H, Gong H, Wu X. Study on adsorption characteristics of uranyl ions from aqueous solutions using zirconium hydroxide. *Journal of Radioanalytical and Nuclear Chemistry*. 2016;308(1):213-20.
- [3] Behin J, Ghadamnan E, Kazemian H. Recent advances in the science and technology of natural zeolites in Iran. *Clay Minerals*. 2019;54(2):131-44.
- [4] Grant DC, Skriba MC, Saha AK. Removal of radioactive contaminants from West Valley waste streams using natural zeolites. *Environmental Progress*. 1987;6(2):104-9.
- [5] Ghasemi MH, Kazemian H, Namdar MA, Malekinezhad A, S.M.R P. Ion exchange behavior of zeolites A and P synthesized by natural clinoptilolite. *Iranian Journal of Chemistry and Chemical Engineering*. 2008;27:111-7.
- [6] Jalali-Rad R, Ghafourian H, Asef Y, Dalir ST, Sahafipour MH, Gharanjik BM. Biosorption of cesium by native and chemically modified biomass of marine algae: introduce the new biosorbents for biotechnology applications. *Journal of Hazardous Materials*. 2004;116(1):125-34.
- [7] Shindo ST STH, Yoshimura N. Development of novel carrier using natural zeolite and continuous ethanol fermentation with immobilized SC in a bioreactor. *Biotechnology Letters*. 2001;23:2001-4.
- [8] Fang X-H, Fang F, Lu C-H, Zheng L. Removal of Cs<sup>+</sup>, Sr<sup>2+</sup>, and Co<sup>2+</sup> Ions from the Mixture of Organics and Suspended Solids Aqueous Solutions by Zeolites. *Nuclear Engineering and Technology*. 2017;49(3):556-61.
- [9] Lan T, Feng Y, Liao J, Li X, Ding C, Zhang D, et al. Biosorption behavior and mechanism of cesium-137 on *Rhodospiridium fluviale* strain UA2 isolated from cesium solution. *Journal of Environmental Radioactivity*. 2014;134:6-13.
- [10] Zinicovscaia I, Safonov A, Boldyrev K, Gundorina S, Yushin N, Petuhov O, et al. Selective metal removal from chromium-containing synthetic effluents using *Shewanella xiamenensis* biofilm supported on zeolite. *Environmental Science and Pollution Research*. 2020;27(10):10495-505.
- [11] Aghadavoud A, Saraee KRE, Shakur HR, Sayyari R. Removal of uranium ions from synthetic wastewater using ZnO/Na-clinoptilolite nanocomposites. *Radiochimica Acta*. 2016;104(11):809-19.
- [12] Bakatula EN, Mosai AK, Tutu H. Removal of uranium from aqueous solutions using ammonium-modified zeolite. *South African Journal of Chemistry*. 2015;68:165-71.
- [13] Fomina M, Gadd GM. Biosorption: current perspectives on concept, definition and application. *Bioresource Technology*. 2014;160:3-14.
- [14] Fadel M, Hassanein NM, Elshafei MM, Mostafa AH, Ahmed MA, Khater HM. Biosorption of manganese from groundwater by biomass of *Saccharomyces cerevisiae*. *HBRC Journal*. 2017;13(1):106-13.
- [15] Saifuddin N, Dinara S. Immobilization of *Saccharomyces cerevisiae* onto cross-linked chitosan coated with magnetic nanoparticles for adsorption of uranium(VI) ions. *Adv Nat Appl Sci*. 2012;6(2):249-67.
- [16] Ayu ED, Halim L, Mellyanawaty M, Sudibyo H, Budhijanto W. The effect of natural zeolite as microbial immobilization media in anaerobic digestion at various concentrations of palm oil mill effluent (POME). *AIP Conference Proceedings*. 2017;1840(1):110005.
- [17] Handley-Sidhu S, Mullan TK, Grail Q, Albadarneh M, Ohnuki T, Macaskie LE. Influence of pH, competing ions and salinity on the sorption of strontium and cobalt onto biogenic hydroxyapatite. *Scientific Reports*. 2016;6(1):23361.
- [18] Zheng XY, Shen YH, Wang XY, Wang TS. Effect of pH on uranium(VI) biosorption and biomineralization by *Saccharomyces cerevisiae*. *Chemosphere*. 2018;203:109-16.
- [19] Emami Moghaddam SA, Harun R, Mokhtar MN, Zakaria R. Potential of Zeolite and Algae in Biomass Immobilization. *BioMed Research International*. 2018;2018:6563196.
- [20] Ma F, Dong B, Gui Y, Cao M, Han L, Jiao C, et al. Adsorption of Low-Concentration Uranyl Ion by Amidoxime Polyacrylonitrile Fibers. *Industrial & Engineering Chemistry Research*. 2018;57(51):17384-93.
- [21] Zhang W, Dong F, Liu M, Song H, Nie X, Huo T, et al. Reduction and Enrichment of Uranium after Biosorption on Inactivated *Saccharomyces cerevisiae*. *Polish Journal of Environmental Studies*. 2020;29(2).
- [22] Peyvandi S, Faghihian H. Biosorption of uranyl ions from aqueous solution by *Saccharomyces cerevisiae* cells immobilized on clinoptilolite. *Journal of Radioanalytical and Nuclear Chemistry*. 2014;301(2):537-43.